

## ISOLATED PHOTON CROSS SECTION MEASUREMENT AT DØ

ASHISH KUMAR\*

*State University of New York at Buffalo  
Buffalo, NY 14260, USA  
E-mail: ashishk@fnal.gov*

We report a new measurement of the isolated photon cross section by the DØ experiment at Fermilab using  $326 \text{ pb}^{-1}$  of data from Run II of the Tevatron. The measured cross section agrees with the theoretical predictions within uncertainties.

### 1. Introduction

Photons originating directly from the hard interaction between partons in hadron collisions provide a clean probe of the hard-scattering dynamics [1]. They are produced mainly via Compton scattering ( $qg \rightarrow q\gamma$ ) or annihilation process ( $q\bar{q} \rightarrow g\gamma$ ). Studies of these direct photons with large transverse momenta,  $p_T^\gamma$ , therefore, offer precision tests of perturbative QCD (pQCD) as well as information on the distribution of gluons in the proton.

DØ has measured the cross section for production of isolated photons using  $326 \text{ pb}^{-1}$  of data. The photons cover central pseudorapidity region  $|\eta| < 0.9$  and span a much wider  $p_T^\gamma$  range (23 to 300 GeV) than Run I measurements [2]. This result has been accepted for publication in Phys. Lett. B [3].

In  $p\bar{p}$  collisions at  $\sqrt{s} = 1.96 \text{ TeV}$  at the Tevatron, the dominant mode of production of photons with  $p_T^\gamma \leq 150 \text{ GeV}$  is the Compton process. Photons from energetic  $\pi^0$  and  $\eta$  mesons are the main background to direct photons especially at small  $p_T^\gamma$ . Since these mesons are produced inside jets, their contribution can be suppressed with respect to direct photons by requiring the photon be isolated from other particles. Isolated electrons from the electroweak production of  $W$  and  $Z$  bosons also contribute to the background at high  $p_T^\gamma$ .

---

\*For the DØ Collaboration.

## 2. Photon Selection

Photons are identified in the DØ detector as isolated energy deposits in the electromagnetic (EM) calorimeter consisting of 4 layers, EM1-EM4. Photon candidates are reconstructed with a simple cone algorithm with cone size  $\mathcal{R} = \sqrt{(\Delta\eta)^2 + (\Delta\phi)^2} = 0.2$ . Candidates are selected if there is significant energy in the EM layers ( $> 95\%$ ), and the probability to have a matched track is less than 0.1%, and they satisfy the isolation requirement  $(E_{total}(0.4) - E_{EM}(0.2))/E_{EM}(0.2) < 0.10$ , where  $E_{total}(0.4)$  and  $E_{EM}(0.2)$  are the total and EM energies within cone size of 0.4 and 0.2, respectively. Potential backgrounds from cosmic rays and leptonic  $W/Z$  boson decays are suppressed by requiring the missing transverse energy to be  $< 0.7p_T^\gamma$ .

## 3. Background Suppression and Photon Purity

Four discriminating variables are used to further suppress the background: the number of EM1 cells with energy  $> 0.4$  GeV within  $\mathcal{R} < 0.2$  and within  $0.2 < \mathcal{R} < 0.4$ , the  $p_T$  sum of tracks within  $0.05 < \mathcal{R} < 0.4$ , and the energy-weighted cluster width in the EM3 layer. They are well modelled in Monte Carlo (MC) and are used to build a neural network (NN) optimized for pattern recognition. The NN is trained to discriminate between direct photons and background events which mainly consists of jets with high EM fractions. The resulting NN output peaks at unity for signal and zero for the background. Events with NN output  $> 0.5$  are retained in the final data sample with 2.7 million photon candidates divided in 17  $p_T^\gamma$  bins.

The photon purity ( $\mathcal{P}$ ) is determined on a statistical basis by fitting the NN distribution in data to a linear combination of the predicted NN distributions for the signal and the background. The distributions of NN output for data, signal MC and background MC are shown in Fig. 1 (left) for the  $44 < p_T^\gamma < 50$  GeV interval. The MC signal and background events here are weighted by the respective fractions that resulted from the fit. The data are well described by the sum of signal and background MC samples, particularly for events with NN output  $> 0.5$ . Photon purities are shown in Fig. 1 (right) as a function of  $p_T^\gamma$ . The purity uncertainty is dominated by MC statistics (EM jets events) at low  $p_T^\gamma$  and data statistics at high  $p_T^\gamma$ . Systematic uncertainties are estimated by using two alternate fitting functions and by varying the number of bins used in the fits. The uncertainty from fragmentation model is estimated by varying the production rate of  $\pi^0$ ,  $\eta$ ,  $K_s^0$ , and  $\omega$  mesons by  $\pm 50\%$ .

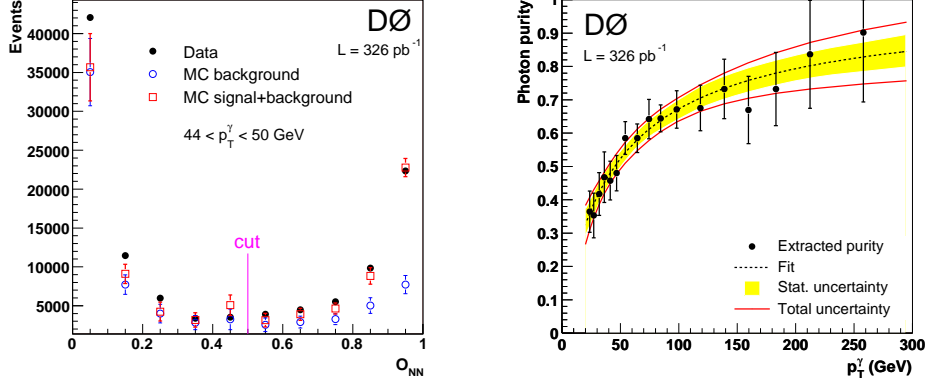


Figure 1. Left) NN output spectra for data ( $\bullet$ ), MC background ( $\circ$ ) and summed MC signal and background ( $\square$ ) for  $44 < p_T^\gamma < 50$  GeV. The MC points are weighted according to the fitted purity (only statistical uncertainties are shown). Right) Photon purity as a function of  $p_T^\gamma$ . The dashed line represents a fit to points, the filled area corresponds to the statistical uncertainty, and the solid lines to the total uncertainty.

#### 4. Isolated Photon Cross Section

The isolated-photon cross section is obtained using the relation:

$$\frac{d^2\sigma}{dp_T d\eta} = \frac{N \mathcal{P} U}{L \Delta p_T^\gamma \Delta \eta A \epsilon} \quad (1)$$

where  $N$  is the number of selected photon candidates,  $L$  is the integrated luminosity,  $A$  is the acceptance,  $\epsilon$  is the selection efficiency, and  $\Delta p_T^\gamma$  and  $\Delta \eta$  are the bin sizes. The factor  $U$  corrects the cross section for the finite resolution of the calorimeter. This unsmearing is performed, as a function of  $p_T^\gamma$ , by iteratively fitting the convolution of an ansatz function with an energy resolution function. Also, the  $p_T^\gamma$  is corrected for the difference in the energy deposited in the material upstream of the calorimeter between electrons (used for the energy calibration) and photons. The measured cross section, together with statistical and systematic uncertainties, is presented in Fig. 2. It can be seen that the cross section falls by about 5 orders of magnitude in the studied  $p_T^\gamma$  range. Statistical uncertainties vary from 0.1% at low  $p_T^\gamma$  to 13.2% at high  $p_T^\gamma$ , while systematic uncertainties range from 11 to 25% and are dominated by that arising from purity estimations. The superimposed theoretical curve corresponds to the next-to-leading order (NLO) pQCD calculation based on JETPHOX [4] using the CTEQ6.1M

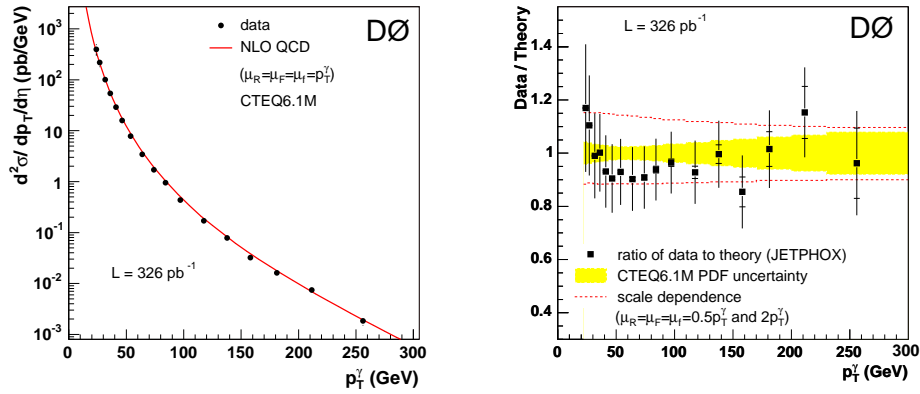


Figure 2. Left) The  $p_T^\gamma$  spectrum of the measured isolated photon cross section. The NLO calculation with JETPHOX is shown as solid line. Right) The ratio of the measured to the predicted cross section. The full vertical line and the internal line correspond to the overall and statistical uncertainty, respectively. Dashed lines represents the effect of scale variations. The shaded region indicates the CTEQ6.1 PDFs uncertainty.

parton distribution functions (PDFs) and all the theoretical scales ( $\mu$ ) set to  $p_T^\gamma$ . Another NLO calculation by Gordon and Vogelsang, based on the small-cone approximation gives consistent results (within 4%). The calculation agrees within uncertainties with the measured cross section in the whole  $p_T^\gamma$  range(Fig. 2). The scale dependence of the predictions is estimated by varying the scales by factors of two. The span of these results is comparable to the overall uncertainty in the measurement. The filled area in Fig. 2 represents the uncertainty associated with the CTEQ6.1M PDFs. The uncertainty from choice of PDFs (MRST2004 /Alekhin2002) is  $< 7\%$ . The difference in shape between data and theory at low  $p_T^\gamma$  is difficult to interpret due to the large theoretical and experimental uncertainties. Higher order calculations are expected to reduce the scale sensitivity and calculations enhanced for soft-gluon contributions are expected to provide better descriptions of the data at low  $p_T^\gamma$ .

## References

1. J. F. Owens, *Rev. Mod. Phys.* **59**, 465 (1987).
2. V. M. Abazov et. al. (DØ collaboration), *Phys. Rev. Lett.* **87**, 251805 (2001).
3. V. M. Abazov et. al. (DØ collaboration), [hep-ex/0511054](#).
4. S. Catani et. al., *JHEP* **05**, 028 (2002).